PNAS RESEARCH ARTICLE | APPLIED BIOLOGICAL SCIENCES

Helminth egg derivatives as proregenerative immunotherapies

David R. Maestas Jr.[a], Liam Chung[a,b], Jin Han[a], Xiaokun Wang[a], Sven D. Sommerfeld[a], Sean H. Kelly[a], Erika Moore[a,c], Helen Hieu Nguyen[a], Joscelyn C. Mejías[a], Alexis N. Peña[a], Hong Zhang[a], Joshua S. T. Hooks[a], Alexander F. Chin[a], James I. Andorko[a,b], Cynthia A. Berlinicke[a], Kavita Krishnan[a], Younghwan Choi[a], Amy E. Anderson[a], Ronak Mahatme[a], Christopher Mejia[a], Marie Eric[a], JiWon Woo[a], Sudipto Ganguly[b,d], Donald J. Zack[e], Liang Zhao[b,d], Edward J. Pearce[b,d,f], Franck Housseau[b,d], Drew M. Pardoll[b,d], and Jennifer H. Elisseeff[a,b,d,1]

Edited by David J. Mooney, Harvard University, Cambridge, MA; received July 19, 2022; accepted January 11, 2023 by Editorial Board Member Rakesh K. Jain

The immune system is increasingly recognized as an important regulator of tissue repair. We developed a regenerative immunotherapy from the helminth *Schistosoma mansoni* soluble egg antigen (SEA) to stimulate production of interleukin (IL)-4 and other type 2-associated cytokines without negative infection-related sequelae. The regenerative SEA (rSEA) applied to a murine muscle injury induced accumulation of IL-4-expressing T helper cells, eosinophils, and regulatory T cells and decreased expression of IL-17A in gamma delta (γδ) T cells, resulting in improved repair and decreased fibrosis. Encapsulation and controlled release of rSEA in a hydrogel further enhanced type 2 immunity and larger volumes of tissue repair. The broad regenerative capacity of rSEA was validated in articular joint and corneal injury models. These results introduce a regenerative immunotherapy approach using natural helminth derivatives.

biomaterials | tissue engineering | regenerative medicine | immune response | helminth

Significance

This work presents a class of regenerative immunotherapies derived from helminth eggs, regenerative soluble egg antigens (rSEAs). rSEA improved wound healing in multiple wound models in part by increasing IL-4-expressing T helper cells and regulatory T cells while decreasing inflammatory IL-17A expression in gamma delta (γδ) T cells. These immunotherapies have the potential to promote wound healing and inhibit fibrosis across multiple tissues and injury types.

Regenerative medicine therapies traditionally aim to promote new tissue development either by stimulating endogenous resident stem cells or through the delivery of exogenous stem cells (1). Biomaterials and biological signals in the form of growth factors or drugs have also been designed and introduced to further enhance cell activity and tissue development. Unfortunately, the efficacy of these therapies often decreases as they move to testing in larger species, and clinical impact remains limited (2). The immune system is now recognized as an important contributor to tissue repair through production of cytokines that stimulate stem cells and creation of a microenvironment that supports new tissue development (3). Multiple immune cells and immunologically active stromal cells contribute to the microenvironment in ways that can inhibit or promote tissue repair. New regenerative medicine therapies that target the immune system may provide an alternative strategy to stimulate tissue repair by creating a proregenerative tissue immune microenvironment. We found previously that acceleration of muscle wound repair by application of extracellular matrix (ECM)-derived biological scaffolds was dependent on induction of T helper type 2 (T_H2) cell responses characterized by the mechanistic target of rapamycin-2 (mTORC2) pathway activation and production of interleukin (IL)-4, and other groups have reported that IL-4-producing eosinophils are also required (4, 5). This discovery prompted us to evaluate the potential for enhanced wound healing by helminthic products since parasitic worm infections are widely regarded to be among the strongest inducers of T_H2 and type 2 immunity.

Parasitic worm infections affect billions of people worldwide, primarily in tropical developing regions, where they can cause morbidity and mortality (6–8). One such parasite, *Schistosoma mansoni*, is a helminth that can infect and can cause severe damage to the liver and hepatic blood vasculature due in part to the immune responses against the eggs lodged in hepatic sinusoids. These responses to xenogeneic foreign bodies and their respective secretome lead to granuloma formation and if left unresolved can result in fibrosis (9–12). While *S. mansoni* and other helminth infections can cause a variety of disease states, they also appear to promote a number of desirable features. For example, some helminth infections reduce the incidence of allergies and are associated with beneficial alterations in the microbiome (13, 14). Infection has also been associated with decreased symptom severity in autoimmune disease and even Alzheimer's disease symptoms, suggesting helminths may induce beneficial immunomodulation (15–17). More directly connecting helminth responses to tissue repair, Nusse et al. demonstrated that a *Heligmosomoides polygyrus* infection triggers epithelial stem cell niche reprogramming, suggesting a connection between helminths and tissue repair that is modulated by the immune response to the worm and its egg secretome (18, 19). Finally, helminth infection induces IL-4 receptor (IL-4R) signaling that down-regulates IL-17A production to benefit rapid tissue repair after the initial infection (20).

Author contributions: D.R.M., D.M.P., and J.H.E. designed research; D.R.M., L.C., J.H., X.W., S.D.S., S.H.K., E.M., H.H.N., J.C.M., A.N.P., H.Z., J.S.T.H., A.F.C., J.I.A., C.A.B., K.K., Y.C., A.E.A., R.M., C.M., M.E., J.W., and L.Z. performed research; L.Z. and E.J.P. contributed new reagents/analytic tools; D.R.M., J.H., X.W., S.G., D.J.Z., F.H., and J.H.E. analyzed data; and D.R.M., D.M.P., and J.H.E. wrote the paper.

Competing interest statement: The authors have organizational affiliations and stock ownership to disclose, J.H.E. holds equity in Unity Biotechnology and Aegeria Soft Tissue and is a consultant for Tessara. D.M.P. is consultant at Aduro Biotech, Amgen, Astra Zeneca, Bayer, Compugen, DNAtrix, Dynavax Technologies Corporation, Ervaxx, FLX Bio, Immunomic, Janssen, Merck, and Rock Springs Capital. D.M.P. holds equity in Aduro Biotech, DNAtrix, Ervaxx, Five Prime therapeutics, Immunomic, Potenza, Trieza Therapeutics. D.M.P. is a member of the scientific advisory board for Bristol Myers Squibb, Camden Nexus II, Five Prime Therapeutics, and WindMil. D.M.P. is a member of board of directors in Dracen Pharmaceuticals.

This article is a PNAS Direct Submission. D.J.M. is a guest editor invited by the Editorial Board.

[1]To whom correspondence may be addressed. Email: jhe@jhu.edu.

This article contains supporting information online at https://www.pnas.org/lookup/suppl/doi:10.1073/pnas.2211703120/-/DCSupplemental.

Published February 13, 2023.

Type 2 immunity is characterized by the influx of T_H2 cells, eosinophils, type 2 innate lymphoid cells, alternatively activated macrophages, and type 2-associated cytokines IL-4, IL-5, IL-9, and IL-13 (18, 21). Previous studies found that the egg secretome components of *S. mansoni* and the soluble egg antigen (SEA) can stimulate type 2 immunity, recapitulating in part the immune response to infection. Evidence suggests that multiple components of SEA can contribute to the type 2 immune responses, in particular the glycoproteins Omega-1 and IL-4-inducing principle of *S. mansoni* eggs (IPSE/alpha-1) and the $Lewis^X$ containing glycan Lacto-N-Fucopentaose III (LNFP III) (22–24).

While the type 2 immune response is historically considered a protective response against parasitic worms, new perspectives suggest that helminths may be co-opting this immune response to repair the damage induced during infection by agonizing type 2 cytokines. For example, IL-4 secreted by eosinophils and T_H2 cells can promote activation of other cell types required for skeletal muscle repair (4, 5). In the central nervous system, IL-4-secreting T_H2 cells promote repair in the retina and spinal cord, and IL-4 levels are positively associated with learning in Alzheimer's disease animal models (25–27). Although helminths drive type 2 responses, it is unknown whether helminth secretory agents can be formulated or engineered as safe and effective regenerative immunotherapies without the pathologies coincident with parasitic infections such as fibrosis and hepatic damage (28–30). In this work, we developed a formulation of SEA from *S. mansoni* eggs that induces a type 2 immune response and promotes tissue repair while decreasing signatures of pathological inflammation and fibrosis, opening the door to a regenerative immunotherapy approach.

Results

Development of a Type 2 Immunotherapy from *S. mansoni* Egg Antigens. The SEA extract from *S. mansoni* is composed of hundreds to thousands of proteins, glycoproteins, and lipids depending on the extraction protocol and is well recognized in its ability to stimulate a type 2 immune response (31–34). We first sought to determine whether SEA could efficiently stimulate a type 2 immune response that would promote tissue repair without deleterious inflammation or fibrosis. *S. mansoni* eggs isolated from infected mice were mechanically disrupted and ultracentrifuged to remove insoluble components to isolate SEA as described by Boros et al. (*SI Appendix*, Fig. S1) (28). We first evaluated the immune response to SEA using an in vitro screen with splenocytes from C57BL/6 wild-type (WT) and IL-4-enhanced green fluorescent protein (eGFP) reporter (4get) mice. Addition of SEA to the splenocyte culture resulted in increased expression of IL-4-eGFP by CD4 T cells comparable to IL-4 (*SI Appendix*, Fig. S2); however, there was also a modest increase in $CD8^+$ T cells expressing interferon-gamma (IFN-γ) as measured by cytokine staining in C57BL/6 splenocyte cultures (*SI Appendix*, Fig. S3). To further test in a wound healing model, we created a volumetric muscle loss (VML) wound in female mice to evaluate the repair capacity of SEA. Application of a single dose of SEA to the VML at the time of injury resulted in a significant increase in *Il4* gene expression in the muscle tissue 1 wk postsurgery (*SI Appendix*, Fig. S4*A*). However, similar to the in vitro studies, there was also a significant increase in inflammatory cytokine expression found in *Ifng, Il1b,* and *Tnfa* in the muscle tissue with SEA treatment compared to saline-treated control injury (*SI Appendix*, Fig. S4*B*).

To determine whether SEA could be formulated to stimulate a dedicated type 2 regenerative immune response without increased interferon-dependent pathological inflammation, we modified the SEA isolation to extract specific layers of the ultracentrifuged egg supernatant. In particular, we further purified the SEA by isolating the lower density soluble fraction and combined it with the lipid portion as recent lipidomic research reported that *S. mansoni* worms and eggs contain proresolving mediators which can promote wound healing (35, 36). Protein gel electrophoresis did not reveal distinct changes in SEA protein composition with the modified isolation protocol (*SI Appendix*, Fig. S5*A*). In contrast, lipid analysis via liquid chromatography–mass spectrometry demonstrated that the modified isolation protocol resulted in a large increase in lipid content (*SI Appendix*, Fig. S5*B*). Further lipidomic analysis revealed changes in the lipid class and individual lipid levels between the standard and modified SEA formulations at both the lipid class and individual lipid levels (*SI Appendix*, Fig. S5 *C* and *D*). The in vitro 4get splenocyte screening assay confirmed IL-4 stimulation along with cell proliferation with the modified SEA formulation (*SI Appendix*, Figs. S5*E* and S6 *A* and *B*) that was consistently generated from multiple batches (*SI Appendix*, Fig. S6 *C* and *D*). Application of the modified SEA formulation to the VML injury model resulted in a significant increase in *Il4* gene expression in the muscle tissue without a concomitant increase in *Ifng* and *Il1b* expression (Fig. 1*A* and *SI Appendix*, Fig. S7*A*). Instead, expression of these inflammatory genes decreased with the modified SEA treatment compared to standard SEA and saline-treated injuries 1 wk postsurgery. Bulk RNA sequencing confirmed significant differences between classical SEA and the modified SEA formulation (*SI Appendix*, Fig. S7*B*). This formulation was then used for all subsequent studies and is referred to as regenerative SEA (rSEA). We then evaluated the different delivery modalities for the rSEA formulation by comparing local and systemic (intraperitoneal, IP) injections. Both local delivery in the VML wound and systemic IP injection of rSEA increased IL-4 expression in the muscle tissue 1 wk after injury (*SI Appendix*, Fig. S8 *A* and *B*). However, further examination of specific immune subsets found that local rSEA treatment significantly increased both IL-4-expressing T cells and eosinophils more than double compared to systemic delivery (*SI Appendix*, Fig. S8*B*), so we used local treatment for all subsequent studies.

rSEA Treatment Increases IL4-Expressing Eosinophils, T_H2 T Cells, and Regulatory T Cells in a VML Injury. Since type 2 immune signals are critical for muscle injury repair, we evaluated the kinetics and cellular sources of IL-4 after rSEA treatment. A single treatment of rSEA at the time of injury increased *Il4* gene expression in the muscle tissue 20- to 30-fold, relative to saline-treated muscles, at 1 wk after surgery (Fig. 1*B*). Treatment with rSEA also increased expression of other type 2-associated genes including *Il5*, *Il13*, and *Gata3* (Fig. 1*B*). Furthermore, the *Il4* gene expression in the draining inguinal lymph nodes (iLNs) increased, peaking at 3 to 7 d after treatment and returning to the level of saline-treated controls after 3 wk (Fig. 1*C*), suggesting that a single rSEA treatment was able to modulate the tissue immune environment for weeks.

Eosinophils are well recognized as a source of IL-4 after muscle injury, so we first evaluated the changes in these cell types after rSEA treatment using multiparametric flow cytometry. Eosinophils ($CD11b^+SiglecF^+SSC^{Hi}$), which depend on type 2 immune cytokines and chemokines such as IL-5 and eotaxin, were the most abundant $CD11b^+$ cell population in the muscle 1 wk post-rSEA treatment, producing an 11-fold increase in the number of cells that remained significantly higher compared to saline-treated controls at 3 wk after treatment (Fig. 1*D*). However, *Il4* gene expression in the muscle tissue still increased in ΔdblGATA [GATA1 knockout (KO)] mice, which lack eosinophils, suggesting that rSEA is stimulating other cell types in the muscle wound (Fig. 1*E*).

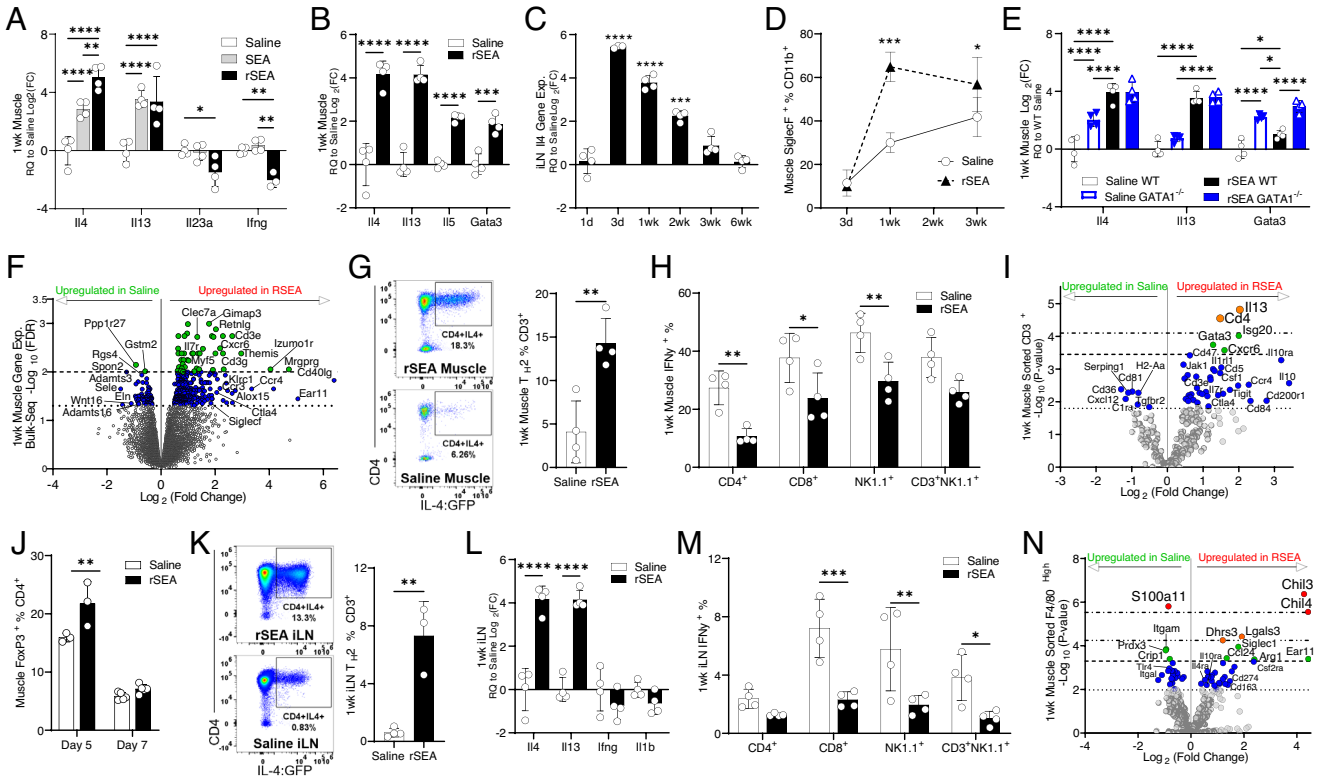

Fig. 1. rSEA treatment promotes a proregenerative type 2 immune microenvironment after muscle injury. Mice had a partial quadriceps resection to create VML injury and received the indicated treatments administered locally at the time of resection. (*A* and *B*) Muscle tissue expression of selected T_H2 and T_H1 genes assessed by qRT–PCR 1 wk after VML and treatment with saline, unfractionated soluble SEA extract and fractionated SEA formulation (regenerative SEA, rSEA). (*C*) *Il4* gene expression of iLNs from VML-injured mice at different time points after rSEA treatment. (*D*) Flow cytometric quantitation of postinjury muscle eosinophils, defined by coexpression of Siglec F and CD11b, over time with rSEA treatment. (*E*) Muscle expression of selected type 2 genes after saline vs. rSEA treatment of WT and GATA1 KO mice. (*F*) Volcano plot of differential expression from bulk RNA sequencing of the muscle 1 wk postinjury and rSEA treatment referenced to saline-treated injuries by the EdgeR analysis. (*G*) Flow cytometry of muscle CD3+CD4+ cells from IL4 reporter (4get) mice treated with either saline or rSEA. (*H*) Muscle IFNγ+ production by various immune cell types assayed by ICS. (*I*) Gene expression profile of sorted CD3+ T cells from the muscle 1 wk postinjury comparing saline and rSEA. (*J*) CD4+Foxp3+ (T_{regs}) in the muscle 5 and 7 d after treatment with either saline or rSEA. (*K*) Flow plots of iLNs from 4get mice draining VML treated 1 wk with saline or rSEA. (*L*) iLN gene expression 1 wk after muscle injury and treatment. (*M*) iLN IFNγ production by various cell types assayed by ICS. (*N*) Gene expression profiling of CD11b+F4/80+Hi macrophages sorted from the muscle 1 wk after saline vs. rSEA treatment. Statistical tests represent all biological replicates, and all experiments excluding (*F*, *I*, and *M*) were replicated at least twice. Graphs show mean ± SD (*A–D*, *G*, *H*, and *J–M*) and mean ± SEM, n = 3 to 5 (*E*). *P < 0.05, **P < 0.01, ***P < 0.001, ****P < 0.0001 by unpaired two-tailed Student's *t* test (*G* and *K*), and two-way ANOVA with Sidak's multiple comparisons. For volcano plot differential expression (*F*, *I*, and *N*), the EdgeR analysis was performed for bulk sequencing FDR (*F*), and sorted cell NanoString analysis FDR values determined by the Benjamini–Yekutieli method (*I* and *N*). Dashed lines (*F*) represent -log10(FDR) < 0.05 and 0.01 and in (*I* and *N*) represent -log10(adjusted *P* value) significance determined by nCounter software (adjusted P < 0.5, 0.1, 0.05, and 0.01, respectively).

At 1 wk after injury, we performed bulk RNA sequencing on the rSEA-treated skeletal muscle and found a wide variety of differential gene expression relative to the saline-treated muscles (Fig. 1*F*). Our bulk sequencing analysis identified 403 differentially expressed genes (330 up-regulated and 73 down-regulated) using the semiconservative EdgeR analysis, with the top up-regulated genes associated with type 2 immunity, natural killer cell activity, T cell activation, antigen processing, and the downregulation of multiple inflammatory genes (*SI Appendix*, Table S1). We also performed a direct comparison of the transcriptional responses to SEA vs. rSEA in the muscle 1 wk after treatment and found notable decreases among multiple inflammatory signatures after rSEA treatment, and we confirmed that most of the type 2 transcriptional responses were alike (*SI Appendix*, Fig. S7*B*). Our comparison of the transcriptional changes influenced by SEA vs. rSEA found that 18 genes were statistically significant at the false discovery rate (FDR) < 0.05 threshold, likely due to the vast similarity between SEA and rSEA. Our direct comparison found that muscles treated with rSEA led to differential expression for up-regulated genes in comparison to SEA treatment, such as *Angptl7*, *Ddit4*, *Klf11*, and *Tsc22d3* which are associated with cell proliferation, lower levels of fibrosis, muscle cell adherence, and responses to IL-10 anti-inflammation. Genes that we found down-regulated in rSEA (up-regulated in SEA) included *Sele* (E-selectin), *Cxcr2* (IL-18RB), *Clec4e*, and *Slfn4* which are associated with reduced trafficking of inflammatory cells and reductions in IL-17A-associated allergy and fibrotic responses mediated by dendritic cell activity. For a discovery-focused analysis of our direct comparison of SEA and rSEA, we further adjusted the FDR threshold and found that many proinflammatory genes were down-regulated specific to rSEA treatment as our qRT–PCR assays had suggested. We then compared the largest differences in transcriptional magnitude between SEA and rSEA treatments when each is referenced to the saline-treated control muscles and found that rSEA trended toward lower expression of inflammatory genes such as *Cxcl5*, *Il1f9* (IL-36γ), *Saa3*, and *Il1b*, higher expression of genes associated with cell proliferation such as *Gsg1* and *Angptl7*, increases in alternatively activated macrophage polarization genes such as *Retnla* and *Cd209e*, and increases of adipose browning genes (*Elovl3*) (*SI Appendix*, Fig. S7*B*).

Previous studies with ECM biomaterials demonstrated that T_H2 cells are critical for the proregenerative response to ECM biological scaffolds, so we further examined the T cell response to rSEA (4, 37, 38). At 1 wk after treatment, $CD3^+$ T cell numbers increased in the muscle wound with $CD3^+CD4^+$ T cells increasing over sevenfold in the muscle with rSEA treatment compared to

saline-treated controls. Treatment with rSEA significantly increased T_H2 [$CD3^+CD4^+GFP^+(IL4^+)$] as a percentage of $CD3^+$ cells in the muscle of 4get mice (Fig. 1*G*). Since the 4get mice report the transcriptional status of the IL-4 locus via GFP expression and have a BALB/c background, we further confirmed direct increases in IL-4 protein with intracellular cytokine staining (ICS) flow cytometry in C57BL/6 mice and found significant increases in T_H2 cells ($CD3^+CD4^+IL4^+$) with rSEA treatment (*SI Appendix*, Fig. S8*C*). There were also changes in the more inflammatory subsets of T cells with rSEA treatment including a significant decrease in the percentage of IFN-γ-expressing $CD4^+$ T cells, a decreased percentage of $CD8^+$ T cells, and a decreased percentage of IFN-γ^+ natural killer and natural killer T cells (Fig. 1*H*), suggesting that rSEA does not induce negative inflammatory changes in addition to the proregenerative response.

We further characterized T cell gene expression changes with rSEA treatment by sorting $CD3^+$ T cells from 1 wk after injury muscle and analyzing gene expression signatures with the NanoString multiplex system. There were 20 genes significantly up-regulated and down-regulated in T cells with rSEA treatment (Fig. 1*I* and *SI Appendix*, Table S2). In particular, rSEA treatment of the muscle wound significantly up-regulated T_H2-associated gene signatures including *Il13, Gata3, and Cd4*. Expression of *Tnfrsf18, Ccr4, Il10,* and *Il10ra* also significantly increased in the T cells after rSEA treatment, suggesting a role for regulatory T cells (T_{regs}). Flow cytometry confirmed a significant increase in T_{regs} ($CD3^+CD4^+Foxp3^+$) in the muscle with rSEA treatment compared to saline controls on days 5 and 7 after injury (Fig. 1*J*) and higher T_{reg} percentages in the lymph nodes draining the muscle injury sites (*SI Appendix*, Fig. S9*A*). As T_{regs} are known to be integral to muscle healing (39), this further supports a regenerative phenotype induced by rSEA.

The draining iLNs also revealed type 2 immune stimulation after rSEA treatment including a significant increase in $IL4^+CD4^+$ T_H2 cell percentage in 4get mice (Fig. 1*K*) and significant increases in T_H2-associated gene expression signatures combined with decreased *Ifng* and *Il1b* at 1 wk after injury (Fig. 1*L*). Similar to the muscle, we further confirmed expression of IL-4 in iLNs with ICS flow cytometry in C57BL/6 mice and found that rSEA induced T_H2 cells ($CD3^+CD4^+IL4^+$, *SI Appendix*, Fig. S9*B*). There was a significant decrease in the percentage of IFN-γ production in $CD4^+$ T cells, a decreased percentage of $CD8^+$ T cells, and a decreased percentage of IFN-γ^+ natural killer and natural killer T cells (Fig. 1*M*). While there were no differences in $CD19^+$ B cells in the muscle 1 wk posttreatment, we found significant changes in B cell percentages and phenotypes in the iLNs (*SI Appendix*, Fig. S10*A*). The number of $CD19^+B220^+$ B cells in the iLNs increased compared to saline controls, and the percentage of $CD19^+B220^+$ B cells also increased in the iLNs (*SI Appendix*, Fig. S10*B*). In the in vitro splenocyte cultures, rSEA exposure significantly increased B cell numbers, suggesting a direct stimulatory role of rSEA on B cells in the regenerative immune response (*SI Appendix*, Fig. S11).

rSEA Induces Alternatively Activated Macrophage Gene Expression in Muscle Wounds. Macrophages are another immune cell type that is central to tissue repair with alternatively activated macrophages associated with productive wound healing (40). The number of macrophages in the muscle tissue had no significant change with rSEA treatment (*SI Appendix*, Fig. S12 *A* and *B*), and there were no differences in CD86 and CD206 expression (*SI Appendix*, Fig. S12*C*). To further evaluate the macrophages, we sorted $CD11b^+F4/80^{Hi+}$ myeloid cells from the muscle wound 1 wk postinjury and utilized the NanoString Myeloid Codeset for gene expression analysis. rSEA treatment induced significant changes in macrophage expression of 57 of the 770 genes tested (Fig. 1*N*). We found that expression of 31 genes significantly increased with rSEA treatment related to metabolism, cell migration/recruitment, and cell activation including *Chil3, Arg1, Cd163, and Ccl24* (Eotaxin-2) that are correlated with noninflammatory macrophages (Fig. 1*N*). Confirming expression of these genes with qRT–PCR, we found that rSEA-treated muscle wounds significantly increased expression of *Chil3, Rnase2a,* and *Arg1* compared to controls (*SI Appendix*, Fig. S12*D*). The $CD11b^+F4/80^{Hi+}$ cells sorted from rSEA-treated muscle also significantly down-regulated several genes associated with inflammation and complement activation genes such as *S100a11*, *Itgam*, *Itgal, Cxcl16*, and *C1qc* (Fig. 1*N* and *SI Appendix*, Table S3). The most strongly down-regulated gene, *Cysltr1,* encodes for cysteinyl leukotriene receptor-1, a potent mediator of allergic inflammation. In contrast to an active helminth infection, rSEA treatment resulted in downregulation of genes such as *Tlr2*, *Tlr4* and *Jun* in the sorted myeloid cells compared to saline-treated controls. This suggests that the rSEA formulation can induce the regenerative components of the type 2 immune helminth response without the deleterious infection response component.

rSEA Stimulation of Type 2 Immunity Correlates with Increased Muscle Repair. IL-4-expressing eosinophils, T_H2 cells, and regulatory T cells are all associated with muscle repair after traumatic injury (4, 5, 39, 41). To assess whether rSEA stimulation of type 2 immunity also benefited muscle repair, we assessed healing and fibrosis with histology and further expression analysis at early (1-wk) and late (6-wk) time points. At 1 wk after surgery time point, where we found broad type 2 immune stimulation, there was a significant increase in expression of genes associated with muscle satellite cell activation (*Pax7, Myod1, Myf5, Myog, Mymk,* and *Areg*) and myofiber fusion and development (*Myh3, Myh8,* and *Myl2*) with rSEA treatment compared to saline-treated controls (Fig. 2*A* and *SI Appendix*, Fig. S12*E*). The increased expression of muscle development genes with rSEA at early time points correlated with increased muscle tissue. At 6 wk after rSEA treatment, immunofluorescent staining of dystrophin, a marker of mature muscle tissue, increased with rSEA treatment compared to saline controls (Fig. 2*B*). Moreover, the rSEA-treated muscle had centrally located nuclei, a characteristic of regenerating muscle tissue, compared to peripheral nuclei in the saline-treated controls. In addition to increased muscle tissue, rSEA treatment reduced fibrosis. Masson's trichrome staining of the muscle injury showed reduced collagen deposition without granuloma formation with rSEA treatment (Fig. 2*B*). While the majority of up-regulated type 2-associated genes had waned by 3 wk after injury and rSEA treatment, we found that the expression of adipose browning genes, *Ucp1* and *Cidea*, had strongly increased at this time range in the muscle (Fig. 2*c*). At 6 wk after injury, we performed functional testing of the injured mice using a treadmill exhaustion assay and found that rSEA treatment led to a significant increase in the running distance achieved by the mice compared to saline vehicle treatment (Fig. 2*D*). Gene expression of the muscle tissue at 6 wk after injury supported the morphological findings with decreased expression of fibrosis-associated genes (*Col1a1*, *Col5a1*, and *Col6a1*) and decreased ratio of *Col1a2* to *Col3a1* with rSEA treatment relative to saline controls (Fig. 2*E*).

rSEA Treatment Decreases IL-17A-Producing $CD4^+$ and $\gamma\delta^+$ T Cells. Schistosome eggs deposited in tissues can induce fibrosis over time and induce granuloma formation similar to the foreign body response. Furthermore, SEA has been used as a model for fibrosis when coated on glass, sepharose, and polystyrene beads in

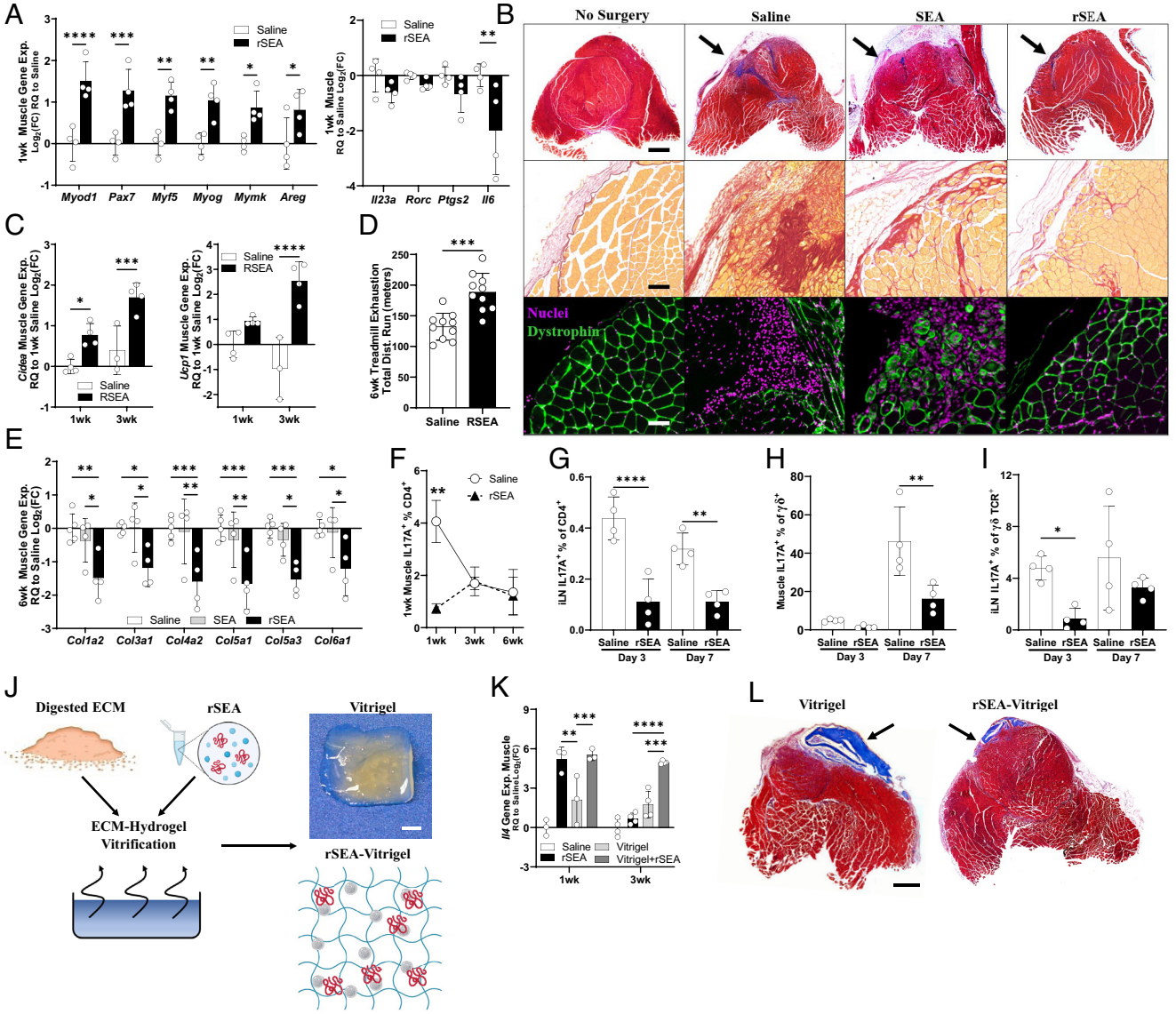

Fig. 2. rSEA promotes skeletal muscle repair and decreases fibrosis and type 3 immune responses. (*A*) One-week postinjury expression of genes involved in muscle regeneration and associated with T_H17 cells in mice treated with saline or rSEA. (*B*) Six-week postinjury muscle histology treated with either saline or rSEA and stained with Masson's trichrome, picrosirius red, and immunofluorescent staining [nuclei = DAPI (purple) and mature muscle = dystrophin (green)]. Arrows indicate site of original muscle resection. (*C*) Muscle gene expression levels of adipose browning-associated genes at 1 and 3 wk after injury and treatment with saline or rSEA. (*D*) Treadmill exhaustion functional testing of mice at 6 wk after injury and treatment with saline or rSEA. (*E*) Gene expression of various fibrosis-associated collagens at 6 wk after injury and treatment with saline or rSEA. (*F*) Percentage of CD4 cells expressing IL-17A at 1, 3, and 6 wk after injury and treatment with saline or rSEA as determined by ICS. (*G*) Percentage of CD4 cells expressing IL-17A by ICS in iLN 1-wk postmuscle injury and treatment with saline or rSEA. (*H*) Percentage of γδ T cells expressing IL-17A in the muscle at 1 wk after injury and treatment. (*I*) Percentage of γδ T cells expressing IL-17A in iLN at 1 wk after injury and treatment with saline or rSEA. (*J*) Production summary and gross image of vitrified SIS-ECM combined with rSEA. (*K*) Gene expression of *Il4* in the muscle for 1, 3, and 6 wk after injury and treatment with saline, rSEA, pure vitrigel, or vitrigel formulated with rSEA. (*L*) Transverse histological sections of muscles stained with Masson's trichrome 6 wk postinjury and treatment with saline, pure vitrigel, or vitrigel formulated with rSEA. Statistical tests represent all biological replicates, and all experiments were replicated at least twice. Graphs show mean ± SD (*A*, *C*–*I*, and *K*), n = 3 to 4. **P* < 0.05, ***P* < 0.01, ****P* < 0.001, and *****P* < 0.0001 by two-way ANOVA with Sidak's multiple comparisons. (Scale bars, 100 μm (*B*), 1 cm (*J*), and 1 mm (*L*).

multiple tissues including the liver and lung (28, 42). As fibrosis and granuloma formation are not desirable outcomes in tissue repair, we therefore sought to further evaluate immunological features associated with fibrosis, specifically type 3 (17) immune cells (43, 44). Expression of type 3 immune-associated genes including *Il23a, Rorc, Ptgs2* (*COX2*), and *Il6* decreased in the muscle tissue 1 wk after injury and rSEA treatment (Fig. 2*A*). IL-17A, central to type 3 immune responses, is implicated in fibrosis in multiple tissues including the lung, liver, and skeletal muscle and in fibrosis associated with the foreign body response (43–46). In parallel with the reduced fibrosis, we observed histologically that rSEA treatment significantly decreased IL-17A-producing T_H17 cell number and percentages in the muscle at day 7 after injury compared to saline, returning to similar levels at 3 and 6 wk (Fig. 2*F*). Further exploring the earlier time points, rSEA induced the most significant decrease in T_H17 cells at 3 d with a significant decrease still present at 7 d after treatment compared to saline (Fig. 2*G*). rSEA treatment also impacted IL-17A expression by γδ T cells (Fig. 2 *H* and *I*). While γδ T cell numbers significantly increased after rSEA treatment at 1 wk (*SI Appendix*, Fig. S13), expression of IL-17A$^+$γδ$^+$ T cells was minimal at 3 d in both groups and significantly decreased with rSEA treatment at 7 d compared to saline-treated controls (Fig. 2 *H* and *I*). In the draining iLN, IL-17A$^+$γδ$^+$ T cell percentage significantly decreased at 3 d with rSEA treatment and moderately decreased at 7 d compared to saline control (Fig. 2*I* and *SI Appendix*, Fig. S13). We also found

a significant reduction in the number of $IL17A^{+}CD4^{+}$ cells (and percentage of CD4 and CD45) of rSEA-treated mice at 1 wk after injury, suggesting that decreased inflammatory signatures are occurring more broadly in regionally and systemically in secondary lymphoid tissues (*SI Appendix*, Fig. S14).

Release of rSEA from a Vitrified ECM Hydrogel Enhances the Type 2 Regenerative Response. Larger tissue defects may require a scaffold to enable cell migration and the repair of larger tissue volumes. Biological scaffolds derived from tissue ECM are used clinically for wound healing and reconstruction applications. Preclinical and clinical studies demonstrate that ECM materials can induce type 2 immune responses and promote tissue repair (37, 47, 48). Although the effects of a single dose of rSEA persist for weeks, the ability to incorporate rSEA into a biomaterial would provide a scaffold for larger tissue defects and deliver the immunotherapy over an extended period of time.

Biological scaffolds based on ECM can be processed into several material forms without compromising their regenerative capacity. Clinically, formulations include powders, sheets, and hydrogels (49). Drugs can also be encapsulated into ECM hydrogels, although these gels are weak and quickly dissolve (38). To create more robust ECM hydrogels that can release proteins and lipids in a controlled manner, we applied a vitrification process that evaporates water in a controlled humidity and temperature so that the macromolecular assembly can occur while a drug or biologic is encapsulated (Fig. 2*J* and *SI Appendix*, Fig. S15*A*). Similar to our previous studies with vitrified collagen, vitrification of urinary bladder-derived ECM produced gels with increased matrix assembly and fiber formation, as visualized by gross histology and transmission electron microscopy (TEM) (*SI Appendix*, Fig. S15*B*) (50, 51). The ECM hydrogel water content decreased after vitrification in parallel with an increase in mechanical properties (G′ modulus) further confirming ECM assembly and formation of a stronger material (*SI Appendix*, Fig. S15*C*). Release profile of a model small-molecule drug from the vitrified ECM confirmed controlled release over 7 d (*SI Appendix*, Fig. S15*D*). Application of ECM particles or vitrigel (without rSEA) induced similar type 2 immune skewing (*SI Appendix*, Fig. S15*F*).

The complex protein and lipid mixture of rSEA makes controlled release difficult to evaluate. Therefore, we sought to evaluate rSEA-encapsulated vitrigels functionally by assessing their impact on wound healing and immune profile skewing. We applied particles of vitrified ECM, with or without encapsulated rSEA, to the murine VML. A single dose of rSEA and rSEA-encapsulated vitrigel stimulated similar levels of *Il4* in the muscle tissue at 1 wk; however, only the vitrigel+rSEA extended the increased *Il4* expression to the 3-wk time point compared to a single dose of rSEA, with a 30-fold increase in *Il4* expression (Fig. 2*K*). The vitrified ECM hydrogel alone stimulated *Il4* gene expression to a small degree. Histological analysis further supported enhanced muscle healing with vitrigel+rSEA treatment without accompanying fibrosis (Fig. 2*L*). The vitrigel ECM provided a scaffold for tissue growth in addition to controlled release of the rSEA that resulted in a larger volume of new muscle tissue. Vitrigels without rSEA are still visible in the muscle after 6 wk compared to vitrigels with rSEA that were largely degraded, likely due to increased repair. Moreover, the overall volume of new muscle tissue was smaller in the vitrigel-alone group.

rSEA Promotes Healing in Articular Cartilage and Corneal Tissue Injury Models. A type 2 immune response and IL-4 expression are associated with repair in multiple tissues beyond the muscle including the liver, articular cartilage, the central nervous system, and the skin (21, 26, 41, 52–54). To determine whether rSEA could be broadly applied to promote regeneration in tissues beyond the muscle, we evaluated the therapeutic potential of rSEA in cartilage and corneal injury models in male mice. For cartilage repair, we used the anterior cruciate ligament transection (ACLT) model that induces articular damage, loss of cartilage, and development of osteoarthritis (55). We injected rSEA intra-articular 2 and 3 wk after the ACLT injury (Fig. 3*A*) and evaluated the joints 4 wk after injury compared to vehicle injections.

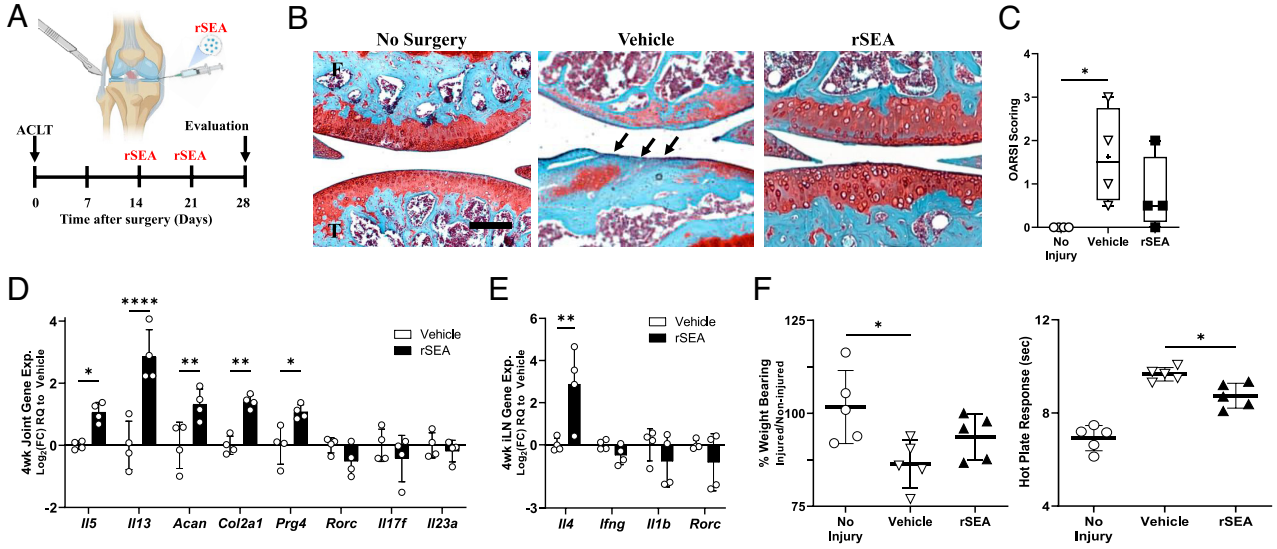

Fig. 3. rSEA immunotherapy promotes repair in articular joint injuries. (*A*) ACLT injury model timeline. (*B*) Representative images from safranin-O stains of uninjured joints (no surgery) or injured joints treated with vehicle or rSEA 4 wk post-ACLT. Arrows indicate where cartilage damage has occurred. (*C*) OARSI scoring of uninjured joints or injured joints treated with vehicle or rSEA 4 wk post-ACLT. (*D*), Articular joint gene expression of type 2, type 3 immune genes, and cartilage ECM genes Aggrecan (*Acan*), type 2 collagen (*Col2a1*), and Lubricin (*Prg4*) 4 wk post-ACLT treated with vehicle or rSEA. (*E*) iLN gene expression of type 2 and type 3 immune genes 4 wk post-ACLT. (*F*) Hot plate reaction times and weight-bearing assessments in mice without injury or 4 wk post-ACLT treated with vehicle (saline) or rSEA. Statistical tests represent all biological replicates, and all experiments were replicated at least twice. Graphs show mean ± SD (*C*–*E*), n = 4 to 5, box and whisker plot with median as central line, and "+" designates mean (*C*). $^{*}P < 0.05$, $^{**}P < 0.01$, $^{***}P < 0.001$, and $^{****}P < 0.0001$ by one-way ANOVA with Tukey's multiple comparisons (*C* and *F*) and two-way ANOVA with Sidak's multiple comparisons (*D* and *E*). (Scale bar, 100 μm (*B*).)

Histological assessment of the articular joint structure and cartilage using safranin-O staining for proteoglycans found that rSEA resulted in higher proteoglycan staining in the cartilage layer, improved tissue structure, and trended in higher levels of repair quality as measured by the semiquantitative OARSI scoring system compared to vehicle controls (Fig. 3 *B* and *C*). Gene expression analysis of the whole joint tissue at the 4-wk time point supported a type 2 immune skewing. Expression of type 2 genes (*Il5* and *Il13*) and cartilage repair and ECM markers (*Prg4*, *Acan1*, and *Col2a1)* increased compared to vehicle controls (Fig. 3*D*). Similar to the muscle injury after rSEA treatment, we found that immune type 1 and type 17 gene expression signatures (*Rorc*, *Il17f*, and *Il23a*) trended downward in comparison to vehicle controls (Fig. 3 *D* and *E*). To evaluate functional repair, we tested nociception and weight bearing of the injured limb. Hot plate nociception measures the latency period of hind limb response to heat-induced pain, wherein shorter time responses indicate lower inflammation and more repair (55). We found that rSEA treatment significantly decreased the nociceptive response time of the mice in comparison to vehicle treatment suggesting reduced pain (Fig. 3*F*). Functional weight-bearing analysis, a measure of the percentage of weight placed upon the injured limb relative to the uninjured limb, improved with rSEA treatment (vehicle: 86.44% and rSEA: 93.61%) (Fig. 3*F*).

We further evaluated the therapeutic potential of rSEA in a corneal wound that is similarly characterized by poor healing capacity and scar formation when damaged. In the corneal debridement injury model, resident stromal cells are activated leading to fibrosis and scarring which results in limited vision (Fig. 4*A*) (56, 57). We injected rSEA in the subconjunctival space immediately after injury and compared the tissue response to control saline injections. Gross imaging of the corneal surface and tissue clarity 2 wk after injury showed a significant increase in corneal repair with rSEA treatment compared to controls as measured by blinded quantitative analysis of the scar area (Fig. 4*B*).

We then examined the immune response in the cornea after wounding and rSEA treatment to see whether an increased type 2 profile correlated with increased tissue repair similar to the muscle and cartilage. We observed few changes in the immune cell populations in the corneal tissue as measured by flow cytometry which may be due to the small cell numbers even when multiple corneas are combined (Fig. 4*C* and *SI Appendix*, Fig. S16*A*). We assessed gene expression of the injured and rSEA-treated corneas and found a significant decrease in inflammatory and angiogenic-associated genes 1 wk posttreatment including *Lyve1, Cd31, Vegfc, Cd36,* and *Acta2* (Fig. 4*D* and *SI Appendix*, Fig. S16*B*). In the draining cervical lymph nodes, however, there was a significant increase in IL-4-expressing $CD4^+$ T cells 1 wk after rSEA treatment and a moderate increase at 2 wk (Fig. 4*E*). In parallel, there was a significant decrease in $IL\text{-}17A^+CD4^+$, $IFN\text{-}\gamma^+CD4^+$, and $IFN\text{-}\gamma^+CD8^+$ T cell percentages with rSEA treatment 1 wk posttreatment with minimal changes at 2 wk (Fig. 4*F*).

Since rSEA treatment increased eosinophil migration in other tissues, we hypothesized that eosinophils may be contributing to rSEA-mediated corneal repair. In the ΔdblGATA model that does not have eosinophils, the scar area significantly increased in size with or without rSEA treatment (Fig. 4*G*). Furthermore, the alpha smooth muscle actin (αSMA) immunofluorescence staining decreased with rSEA treatment in WT mice, but we found that this increased with or without treatment in eosinophil-deficient mice (ΔdblGATA), suggesting impaired wound healing and increased fibrosis (Fig. 4*H*). Immunological analysis of the draining cervical lymph node revealed that the significant increase in T_H2 cells induced by rSEA in WT animals is completely ablated in ΔdblGATA mice (Fig. 4*I*). This finding contrasts with the VML model (Fig. 1*E*) and thus suggests that eosinophils are important effectors in healing of the corneal wound by rSEA-induced T_H2 responses. Thus, rSEA treatment acts on multiple cell types, whose importance in the regenerative process depends on the tissue type and wound.

In this work, we designed a proregenerative immunotherapy derived from fractionated helminth parasite egg antigens and demonstrate their ability to enhance wound healing and deter fibrosis post-traumatic injury across three injury models. Taking the eggs from *S. mansoni* helminths, we derived an alternative formulation from the SEA, rSEA. We showed that the rSEA stimulated a type 2 immune signature in lymphoid cells and myeloid cells, further decreasing proinflammatory immune polarization, and later time points revealed decreased levels of fibrosis associated with inhibition of T_H17 and $\gamma\delta^+IL\text{-}17A^+$ cells. Application of rSEA to the muscle, the cornea, and articular joint injuries generally improved tissue healing assessed by gene expression signatures, cell populations, and/or histological assessment. Controlled release of rSEA from a natural sourced and decellularized biomaterial hydrogel further promoted healing and regeneration of larger tissue volumes. Our rSEA formulation, particularly in the form of an ECM hydrogel, is therefore a regenerative immunotherapy with potentially broad application to tissue repair and homeostasis, although several vital questions remain for exploration in future work such as the optimal formulations and scaling of SEA to benefit healing, deleterious off-target effects, and immunotherapy-induced susceptibility to other pathogens during treatment.

Discussion

A type 2 immune response is central to how the immune system responds to helminth infection. While the type 2 response has long been considered an antihelminth response, it is also now hypothesized that helminths may induce this anti-inflammatory immune signature to repair the damage caused to the host, thereby enhancing mutual survival. Recent studies highlight the importance of the context of expression of type 2-associated molecules that are important in dictating outcomes, such as amphiregulin, IL-13, and IL-33 (20). IL-4 and type 2 immunity are associated with tissue repair and healing in multiple tissue types including the liver (52), the bone (53), cartilage (48), and the muscle (4, 5) and corneal (57) and nervous (26, 54) tissues, suggesting that rSEA may be broadly applicable for tissue repair (18, 20, 21). Treatment with rSEA induced an immune profile that included eosinophils and T_H2 cells producing significantly higher levels of IL-4, IL-5, and IL-13 protein or gene expression compared to injured tissue without treatment. The type of tissue where injury and treatment may impact which cells are responding to rSEA and promoting tissue repair. In our studies, application of rSEA to a corneal wound in the ΔdblGATA murine corneal injury model completely abolished repair. However, in skeletal muscle injuries, the ΔdblGATA mice did not ablate prohealing gene expression signatures induced by rSEA despite their well-recognized role in muscle tissue repair (5). This suggests that rSEA may activate multiple immune cell populations to promote repair that differ according to tissue type. It is also likely that rSEA influences stromal, stem, or progenitor cell populations in addition to immune cells as helminth infections were shown to stimulate stem cells in the intestinal niche (19).

As type 2 immune responses have also been implicated in long-term fibrotic and allergic responses (21), further studies may elucidate how these immune responses differ from the regenerative response. Chronic helminth exposure results in fibrosis and is

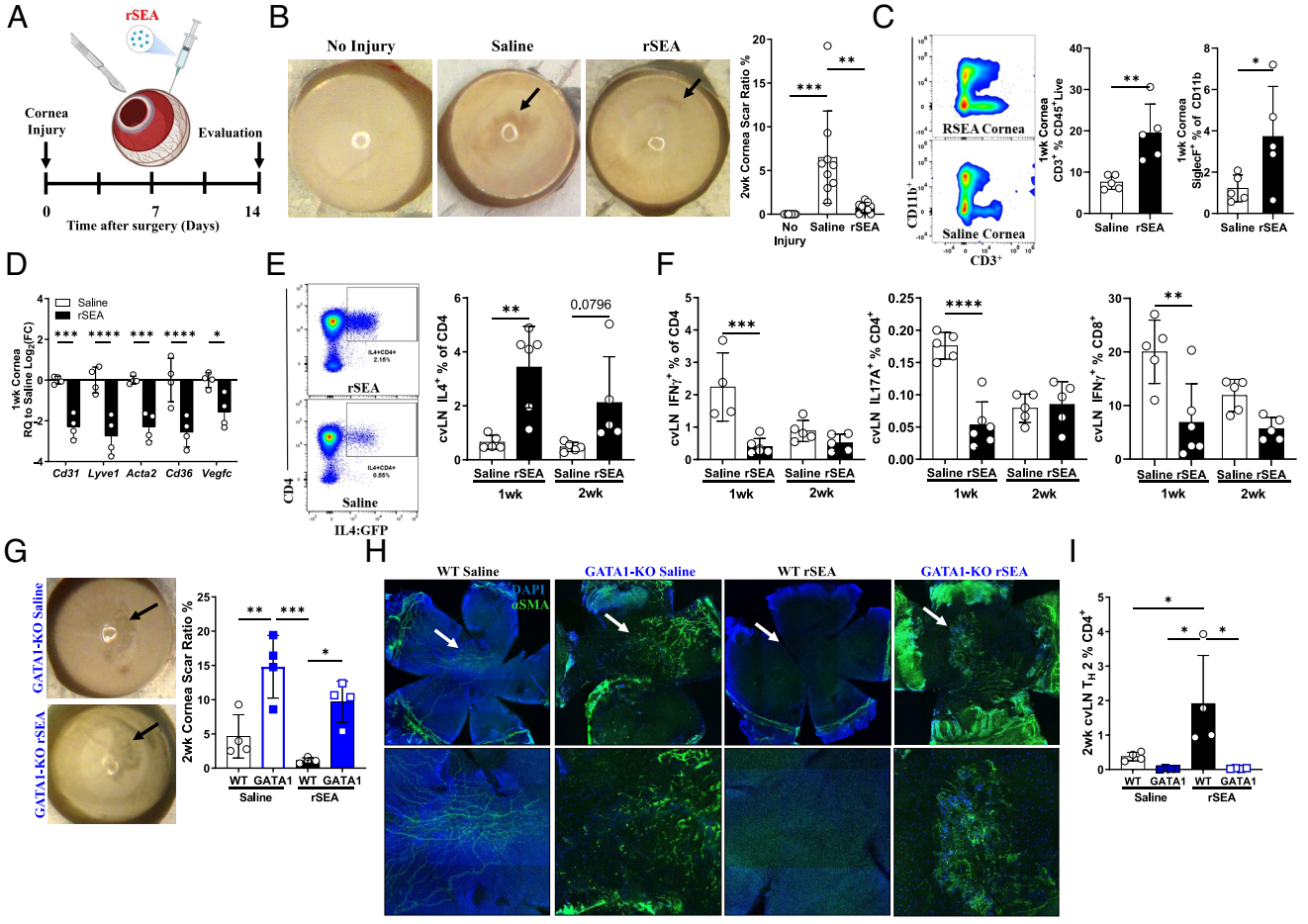

Fig. 4. rSEA immunotherapy promotes repair in corneal injury. (*A*) Corneal debridement injury model timeline. (*B*) Corneal gross images and scar ratio assessment at 2 wk after injury treated with saline vehicle or rSEA, two study replications combined. (*C*) Flow cytometry populations isolated from the cornea 1 wk postinjury and treatment with saline or rSEA. (*D*) Corneal expression of genes associated with scar vascularization at 1 wk after injury and treatment with saline or rSEA. (*E*) Representative flow plots of 2 wk after injury 4get cervical LNs (cvLN) and % T_H2 populations at 1 wk vs. 2 wk after injury and treatment with saline or rSEA. (*F*) ICS from cvLN of T_H1, T_H17, and IFNγ$^+$CD8$^+$ T cells (%) at 1 and 2 wk after injury and treatment with saline or rSEA. (*G*) Representative gross images of wounded corneas from GATA1 KO mice treated 2 wk with saline or rSEA and scar area ratio assessment. (*H*) Immunofluorescent staining of nuclei (DAPI, blue) and α-SMA (green) on corneas 2 wk postinjury and treatment with saline or rSEA in WT vs. GATA1 KO mice. (*I*) cvLN ICS for IL-4 in WT vs. GATA1 KO mice 2 wk postinjury and treatment with saline or rSEA. Statistical tests represent all biological replicates, and all experiments were replicated at least twice. Graphs show mean ± SD (*B–F*, *G*, and *I*), n = 4 to 6. *P < 0.05, **P < 0.01, ***P < 0.001, and ****P < 0.0001 by one-way ANOVA with Tukey's multiple comparisons (*B*) and two-way ANOVA with Sidak's multiple comparisons (*D–F*, *G*, and *I*).

postulated to be from an overzealous wound healing response (18, 21). The mechanical properties of worm casings and the secretions from the eggs together may also contribute to helminth-related fibrosis as we observed with biomaterial hydrogels with increasing stiffness that produced more fibrosis in part due to IL-17 signaling (42). Recently, it was found that *S. mansoni* eggshells alone can temporarily deter the foreign body response and that the antigens secreted through the eggshell induce granulomas to control the timing of egg extrusion into the environment to continue the parasite's life cycle (42). In our regenerative studies with the rSEA therapy, we did not observe fibrosis and instead found a reduction in IL-17 and fibrosis markers.

Sex differences in immune responses contribute to autoimmune disease, infection, and vaccine responses. While sex differences in the immune response to tissue damage and contributions to repair are likely, these differences are not well studied and currently remain largely unknown. In our studies, we tested the rSEA response in a muscle injury in female mice and the articular and corneal injuries in male mice so they could be compared to previous work in the respective fields (58–61). The rSEA treatment improved tissue repair in both male and female mice in their specific injuries. Understanding sex-specific responses to tissue damage, that may be unique and specific to a particular tissue or organ, along with differences in therapeutic response to a regenerative immunotherapy will need to be further elucidated.

While we purified SEA to make the regenerative formulation, it is still a complex mixture of proteins, proteoglycans, and lipids. Multiple components of SEA have been identified, and the known functions of these individual components support their potential in promoting tissue repair. It is likely that the different components of rSEA target different and complementary cellular functions in the immune and stromal compartments of a wound and tissue to stimulate type 2 immune responses and tissue repair. The differences in immune modulation induced by rSEA compared with SEA, along with the increased lipid levels we observed in rSEA, suggest that the lipid component is an important contributor to the reduced inflammation and increased tissue repair. Multiple classes of lipids, including resolvins, protectins, and maresins, have known roles in mediating inflammation and promoting tissue repair (62).

While further analysis may identify distinct roles for individual components of SEA, further isolation of SEA and reduction to a single agent and mechanism could reduce the overall therapeutic response. ECM-derived biomaterials are an example of a complex

mixture where a mixture of components contribute to the therapeutic efficacy. Multiple ECM-derived materials are Food and Drug Administration (FDA) approved as medical devices and biologics depending on the source and clinical application. Manufacturing protocols and biological release assays enable consistent products that have a strong track record of safety and efficacy. As in vitro culture of *Schistosomiasis* has already been demonstrated (63), reproducible culture and scale-up may be possible. Taken together, the development of rSEA and the tissue repair findings describe a regenerative medicine approach that targets the immune system and presents a class of immunotherapies with potential broad application across multiple tissue and organ systems.

Data, Materials, and Software Availability. A dedicated effort was made to adhere to conventional standards for all studies herein to ensure reproducibility. All *S. mansoni* eggs, livers, and reagents utilized in this work were obtained courtesy of the Biomedical Research Institute (BRI) (Rockville), a 501 (c) (3) nonprofit research company supported by the National Institute of Allergy and Infectious Diseases (NIAID) of the NIH through the NIH–NIAID, contract: HHSN272201700014I.

ACKNOWLEDGMENTS. We thank the BRI of Rockville, Maryland, for providing helminth eggs and SEA-associated resources, contract: HHSN272201700014I, and Christopher A. Moad for technical assistance. Funding: This study was funded by NIH Pioneer Award DP1AR076959 (J.H.E.), Bloomberg~Kimmel Institute (J.H.E., D.M.P.), Morton Goldberg Professorship (J.H.E.), The Department of Defense, award number W81XWH-19-1-0576 (J.H.E.), The National Eye Institute grant, R01EY029055 (J.H.E.), The NSF Graduate Research Fellowship Program #DGE-1746891 (D.R.M., A.N.P.), The Armed Forces Institute for Regenerative Medicine II award number WFUHS 441081 CF-11 (J.H.E.), The NIH T32 Training Grant 1T32AG058527-01 (J.I.A.), The NIH T32 Training Grant 5T32CA153952-08 (J.I.A.), The NIH K-Award 1KL2TR001429 (E.M.), and The Rhines Rising Star Larry Hench Professorship (E.M.).

Author affiliations: [a]Translational Tissue Engineering Center, Johns Hopkins University, Baltimore, MD 21287; [b]Bloomberg~Kimmel Institute for Cancer Immunotherapy, Johns Hopkins University, School of Medicine, Baltimore, MD 21287; [c]Materials Science and Engineering, University of Florida, Gainesville, FL 32611; [d]Department of Oncology and Sidney Kimmel Comprehensive Cancer Center, Johns Hopkins University School of Medicine, Baltimore, MD 21287; [e]Department of Ophthalmology, Wilmer Eye Institute, Johns Hopkins University School of Medicine, Baltimore, MD 21287; and [f]Department of Molecular Microbiology and Immunology, Johns Hopkins University Bloomberg School of Public Health, Baltimore, MD 21287

1. T. E. G. Krueger, D. L. J. Thorek, S. R. Denmeade, J. T. Isaacs, W. N. Brennen, Concise review: Mesenchymal stem cell-based drug delivery: The good, the bad, the ugly, and the promise. *Stem Cells Transl Med.* **7**, 651–663 (2018).
2. C. Chabannon *et al.*, Hematopoietic stem cell transplantation in its 60s: A platform for cellular therapies. *Sci. Transl Med.* **10**, eaap9630 (2018).
3. P. Laurent *et al.*, Immune-mediated repair: A matter of plasticity. *Front. Immunol.* **8**, 454 (2017).
4. K. Sadtler *et al.*, Developing a pro-regenerative biomaterial scaffold microenvironment requires T helper 2 cells. *Science* **352**, 366–370 (2016).
5. J. E. Heredia *et al.*, Type 2 innate signals stimulate fibro/adipogenic progenitors to facilitate muscle regeneration. *Cell* **153**, 376–388 (2013).
6. D. G. Colley, A. L. Bustinduy, W. E. Secor, C. H. King, Human schistosomiasis. *Lancet* **383**, 2253–2264 (2014).
7. D. P. McManus *et al.*, *Seminars in Immunopathology* (Springer, 2020), **vol. 42**, pp. 355–371.
8. T. Vos *et al.*, Years lived with disability (YLDs) for 1160 sequelae of 289 diseases and injuries 1990–2010: A systematic analysis for the Global Burden of Disease Study 2010. *Lancet* **380**, 2163–2196 (2012).
9. M. L. Burke *et al.*, Immunopathogenesis of human schistosomiasis. *Parasite Immunol.* **31**, 163–176 (2009).
10. B. B. Graham, A. P. Bandeira, N. W. Morrell, G. Butrous, R. M. Tuder, Schistosomiasis-associated pulmonary hypertension: Pulmonary vascular disease: The global perspective. *Chest* **137**, 20S–29S (2010).
11. B. J. Vennervald *et al.*, Detailed clinical and ultrasound examination of children and adolescents in a Schistosoma mansoni endemic area in Kenya: Hepatosplenic disease in the absence of portal fibrosis. *Trop. Med. Int. Health* **9**, 461–470 (2004).
12. K. S. Warren, A. A. Mahmoud, P. Cummings, D. J. Murphy, H. B. Houser, Schistosomiasis mansoni in Yemeni in California: Duration of infection, presence of disease, therapeutic management. *Am. J. Trop Med. Hyg.* **23**, 902–909 (1974).
13. T. P. Brosschot, L. A. Reynolds, The impact of a helminth-modified microbiome on host immunity. *Mucosal Immunol.* **11**, 1039–1046 (2018).
14. T. P. Jenkins *et al.*, Schistosoma mansoni infection is associated with quantitative and qualitative modifications of the mammalian intestinal microbiota. *Sci. Rep.* **8**, 1–10 (2018).
15. R. M. Maizels, Regulation of immunity and allergy by helminth parasites. *Allergy* **75**, 524–534 (2020).
16. C. W. Su *et al.*, Helminth-induced and Th2-dependent alterations of the gut microbiota attenuate obesity caused by high-fat diet. *Cell Mol. Gastroenterol. Hepatol.* **10**, 763–778 (2020).
17. M. M. Zaiss, N. L. Harris, Interactions between the intestinal microbiome and helminth parasites. *Parasite Immunol.* **38**, 5–11 (2016).
18. W. C. Gause, T. A. Wynn, J. E. Allen, Type 2 immunity and wound healing: Evolutionary refinement of adaptive immunity by helminths. *Nat. Rev. Immunol.* **13**, 607–614 (2013).
19. Y. M. Nusse *et al.*, Parasitic helminths induce fetal-like reversion in the intestinal stem cell niche. *Nature* **559**, 109–113 (2018).
20. F. Chen *et al.*, An essential role for TH 2-type responses in limiting acute tissue damage during experimental helminth infection. *Nat. Med.* **18**, 260–266 (2012).
21. R. L. Gieseck III, M. S. Wilson, T. A. Wynn, Type 2 immunity in tissue repair and fibrosis. *Nat. Rev. Immunol.* **18**, 62 (2018).
22. B. Everts *et al.*, Omega-1, a glycoprotein secreted by Schistosoma mansoni eggs, drives Th2 responses. *J. Exp. Med.* **206**, 1673–1680 (2009).
23. M. Okano, A. R. Satoskar, K. Nishizaki, D. A. Harn, Lacto-N-fucopentaose III found on Schitosoma mansoni egg antigens functions as adjuvant for proteins by inducing Th2-type response. *J. Immunol.* **167**, 442–450 (2001).
24. G. Schramm *et al.*, Cutting edge: IPSE/alpha-1, a glycoprotein from Schistosoma mansoni eggs, induces IgE-dependent, antigen-independent IL-4 production by murine basophils in vivo. *J. Immunol.* **178**, 6023–6027 (2007).
25. T. Kiyota *et al.*, CNS expression of anti-inflammatory cytokine interleukin-4 attenuates Alzheimer's disease-like pathogenesis in APP+PS1 bigenic mice. *FASEB J.* **24**, 3093–3102 (2010).
26. X. Liu *et al.*, Interleukin-4 is essential for microglia/macrophage M2 polarization and long-term recovery after cerebral ischemia. *Stroke* **47**, 498–504 (2016).
27. A. Quarta, Z. Berneman, P. Ponsaerts, Neuroprotective modulation of microglia effector functions following priming with interleukin 4 and 13: Current limitations in understanding their mode-of-action. *Brain Behav. Immun.*, 856–866 (2020).
28. D. L. Boros, K. S. Warren, Delayed hypersensitivity-type granuloma formation and dermal reaction induced and elicited by a soluble factor isolated from Schistosoma mansoni eggs. *J. Exp. Med.* **132**, 488–507 (1970).
29. D. Ditgen *et al.*, Harnessing the helminth secretome for therapeutic immunomodulators. *Biomed. Res. Int.* **2014**, 964350 (2014).
30. M. M. Harnett, W. Harnett, Can parasitic worms cure the modern world's ills? *Trends Parasitol.* **33**, 694–705 (2017).
31. M. Giera *et al.*, The Schistosoma mansoni lipidome: Leads for immunomodulation. *Anal. Chim. Acta* **1037**, 107–118 (2018).
32. J. Jang-Lee *et al.*, Glycomics analysis of Schistosoma mansoni egg and cercarial secretions. *Mol. Cell Proteomics* **6**, 1485–1499 (2007).
33. W. Mathieson, R. A. Wilson, A comparative proteomic study of the undeveloped and developed Schistosoma mansoni egg and its contents: the miracidium, hatch fluid and secretions. *Int J Parasitol.* **40**, 617–628 (2010).
34. C. L. Cass *et al.*, Proteomic analysis of Schistosoma mansoni egg secretions. *Mol. Biochem. Parasitol.* **155**, 84–93 (2007).
35. M. C. Basil, B. D. Levy, Specialized pro-resolving mediators: endogenous regulators of infection and inflammation. *Nat. Rev. Immunol.* **16**, 51–67 (2016).
36. J. F. Markworth *et al.*, Resolvin D1 supports skeletal myofiber regeneration via actions on myeloid and muscle stem cells. *JCI Insight* **5**, e137713 (2020).
37. K. C. Sasse, D. L. Warner, D. Ackerman, J. Brandt, Parastomal hernia repair with urinary bladder matrix grafts: A case series. *Int. J. Case Rep. Images* **7**, 85–91 (2016).
38. R. M. Wang, K. L. Christman, Decellularized myocardial matrix hydrogels: In basic research and preclinical studies. *Adv. Drug Deliv. Rev.* **96**, 77–82 (2016).
39. D. Burzyn *et al.*, A special population of regulatory T cells potentiates muscle repair. *Cell* **155**, 1282–1295 (2013).
40. D. M. Mosser, J. P. Edwards, Exploring the full spectrum of macrophage activation. *Nat. Rev. Immunol.* **8**, 958–969 (2008).
41. V. Salmon-Ehr *et al.*, Implication of interleukin-4 in wound healing. *Lab. Invest.* **80**, 1337–1343 (2000).
42. K. K. Takaki, G. Rinaldi, M. Berriman, A. J. Pagan, L. Ramakrishnan, Schistosoma mansoni eggs modulate the timing of granuloma formation to promote transmission. *Cell Host Microbe* **29**, 58–67.e55 (2021).
43. L. Chung *et al.*, Interleukin 17 and senescent cells regulate the foreign body response to synthetic material implants in mice and humans. *Sci. Transl. Med.* **12**, eaax3799 (2020).
44. T. Fabre *et al.*, Type 3 cytokines IL-17A and IL-22 drive TGF-beta-dependent liver fibrosis. *Sci. Immunol.* **3**, eaar7754 (2018).
45. M. G. Shainheit *et al.*, The pathogenic Th17 cell response to major schistosome egg antigen is sequentially dependent on IL-23 and IL-1β. *J. Immunol.* **187**, 5328–5335 (2011).
46. K. Ramani, P. S. Biswas, Interleukin-17: Friend or foe in organ fibrosis. *Cytokine* **120**, 282–288 (2019).
47. J. Dziki *et al.*, An acellular biologic scaffold treatment for volumetric muscle loss: Results of a 13-patient cohort study. *NPJ Regen. Med.* **1**, 16008 (2016).
48. P. Bettiol, C. Cox, C. Gerzina, J. Simpson, B. MacKay, Novel use of a porcine bladder extracellular matrix scaffold to treat postoperative seroma in a total knee arthroplasty patient. *Arthroplasty today* **7**, 143–147 (2021).
49. M. T. Spang, K. L. Christman, Extracellular matrix hydrogel therapies: In vivo applications and development. *Acta Biomater.* **68**, 1–14 (2018).
50. X. Wang *et al.*, Multifunctional synthetic Bowman's membrane-stromal biomimetic for corneal reconstruction. *Biomaterials* **241**, 119880 (2020).
51. X. Wang *et al.*, Collagen vitrigels with low-fibril density enhance human embryonic stem cell-derived retinal pigment epithelial cell maturation. *J. Tissue Eng. Regen. Med.* **12**, 821–829 (2018).
52. Y. P. Goh *et al.*, Eosinophils secrete IL-4 to facilitate liver regeneration. *Proc. Natl. Acad. Sci. U.S.A.* **110**, 9914–9919 (2013).

53. L. Gong *et al.*, An interleukin-4-loaded bi-layer 3D printed scaffold promotes osteochondral regeneration. *Acta Biomater.* **117**, 246–260 (2020).
54. J. Yang *et al.*, Interleukin-4 ameliorates the functional recovery of intracerebral hemorrhage through the alternative activation of microglia/macrophage. *Front. Neurosci.* **10**, 61 (2016).
55. M. Z. Ruan, R. M. Patel, B. C. Dawson, M. M. Jiang, B. H. Lee, Pain, motor and gait assessment of murine osteoarthritis in a cruciate ligament transection model. *Osteoarthritis Cartilage* **21**, 1355–1364 (2013).
56. M. A. Stepp *et al.*, Wounding the cornea to learn how it heals. *Exp. Eye Res.* **121**, 178–193 (2014).
57. X. Wang *et al.*, Type 2 immunity induced by bladder extracellular matrix enhances corneal wound healing. *Sci. Adv.* **7**, eabe2635 (2021).
58. B. A. Christiansen *et al.*, Non-invasive mouse models of post-traumatic osteoarthritis. *Osteoarthritis and cartilage* **23**, 1627–1638 (2015).
59. S. M. Greising, B. T. Corona, C. McGann, J. K. Frankum, G. L. Warren, Therapeutic approaches for volumetric muscle loss injury: A systematic review and meta-analysis. *Tissue Eng. Part B: Rev.* **25**, 510–525 (2019).
60. T. Histing *et al.*, Small animal bone healing models: Standards, tips, and pitfalls results of a consensus meeting. *Bone* **49**, 591–599 (2011).
61. S. L. Klein, K. L. Flanagan, Sex differences in immune responses. *Nat. Rev. Immunol.* **16**, 626–638 (2016).
62. C. N. Serhan, B. D. Levy, Resolvins in inflammation: Emergence of the pro-resolving superfamily of mediators. *J. Clin. Invest.* **128**, 2657–2669 (2018).
63. S. Frahm *et al.*, A novel cell-free method to culture Schistosoma mansoni from cercariae to juvenile worm stages for in vitro drug testing. *PLoS Negl. Trop. Dis.* **13**, e0006590 (2019).